

## Modal interaction of power systems with high penetration of renewable energy and BES systems



Herlambang Setiadi<sup>a</sup>, Awan Uji Krismanto<sup>a</sup>, N. Mithulananthan<sup>a,\*</sup>, M.J. Hossain<sup>b</sup>

<sup>a</sup> School of Information Technology & Electrical Engineering, The University of Queensland, Brisbane, Australia

<sup>b</sup> Department of Engineering, Macquarie University Sydney, NSW 2109, Australia

### ARTICLE INFO

#### Keywords:

Modal interaction  
Low-frequency oscillation  
RESs  
BES system

### ABSTRACT

Integration of renewable energy sources (RESs) at transmission level is getting popular in the recent years. RESs have advantages of generating clean and environmentally friendly electricity. However, due to the uncertainty and less inertia characteristic of the RESs based power plant, it can bring negative impacts on small signal stability which is also known as low-frequency oscillatory stability. Hence, utilizing an additional device, such as battery energy storage (BES) in power system with high penetration of RESs is inevitable. BES system could provide additional active power to the grid to overcome the shortfall energy from RESs. Conversely, BES installation may also introduce negative impact on system dynamic in terms of possible interaction with other elements of the power system. Therefore, proper gain control setting of BES is required to avoid undesirable interaction and make sure system stability. This paper investigates the impact of gain variation in BES controller to oscillatory stability and modal interaction on the power system. Eigenvalue trajectories, participation factor and time domain simulation of the critical modes are thoroughly investigated. Influence of the capacity of BES and its location on damping ratio of weak modes is also examined in the paper. Moreover, the mitigation of modal interaction occurrence through BES gain tuning using metaheuristic algorithms is proposed in this paper. From the simulation results, it was found that increasing BES's gain controller could lead to the interaction events. It was also reported that the proposed tuning method is feasible to mitigate the occurrence of modal interaction.

### 1. Introduction

In the last decade, the requirement of clean energy to minimize fossil fuels and green gas emission has led to the global integration of RESs [1]. Leading countries such as Canada, China, Denmark, Germany, Japan, UK, and the USA have set a massive target for increasing penetration level of RESs. Moreover, other countries are also following this path for integrating RESs, either as islanded or integrated into distribution and transmission levels. Among numerous type of RESs, solar and wind are the popular sources to produce electricity in the significant amount [1] due to its flexibility and technologies developments.

Although RESs based on solar (PV) and the wind are promising a large positive impact on the environment and economy, it may bring negative impacts to the grid operation. The majority of RESs based on wind and PV utilise power electronic devices, such as a DC/AC, AC/DC, and DC/DC converters as power conversion devices. The new power electronic based converter and the dynamics of RESs power plants might deteriorate power systems stability, particularly in low-frequency

oscillation. Moreover, the intermittent and uncertainties power output of RESs have become the main concern in power system stability [2,3].

PV and wind energy conversion system (WECS) have a significant impact in low-frequency oscillation as reported in previous research [4–6]. The possible impact of integrating WECS in power system oscillatory stability is presented in [4,5]. It was noticeable that high penetration of WECS might either improve or worsen the damping of the critical eigenvalue. The influence of PV plants in low-frequency oscillation was reported in [6]. It was reported that damping performance of the power system decreased when a large-scale PV plants were integrated into the grid.

The oscillatory condition in power system could become worse due to a high penetration of RESs. Conventionally, power system stabilizer (PSS) is responsible for controlling the oscillatory circumstances. However, with high penetration of RESs, those device is not sufficient to handle the oscillatory concern. Hence, utilizing an additional device such as BES system should be considered to improve the dynamic performance of power system. The implementation of BES to enhance power system operation has been investigated extensively.

\* Corresponding author.

E-mail address: [mithulan@tee.uq.edu.au](mailto:mithulan@tee.uq.edu.au) (N. Mithulananthan).

Implementation of BES system for load frequency control is presented in [7,8]. It was found that by utilizing BES system, the settling time and overshoot of the frequency can be accelerated and reduced respectively. It was also found that BES system provides a satisfactory solution for voltage control and peak shaving as reported in [9,10]. Furthermore, BES system could be implemented to support system damping as presented in [11,12]. Although BES system can provide positive impact as reported above, it introduces a significant influence on dynamic modal behavior, which may result in interaction events in power system. Hence, the main contribution of this paper are:

- Examining the influence of BES on small signal stability performance.
- Investigating potential interaction between various modes in BES Systems.
- Analyzing the impact of large scale wind energy and large scale PV plants on the small signal stability of power system with BES system.
- Optimizing BES control gain using differential evolution algorithm to maximize damping and minimizing interactions with other modes.

The rest of the paper is organized as follows: Section 2 provides a dynamic model of a power system including WECS, large-scale PV plant, and BES system models. Section 3 briefly explain low-frequency oscillation and power system interaction. Eigenvalue trajectories, participation factor and time domain simulation are presented in Section 4. Section 5 highlights the contribution, conclusions and future directions of the research.

## 2. Fundamental theory

### 2.1. Wind energy conversion system model

WECS model considered in this research comprises of wind turbine model, permanent magnet synchronous generator (PMSG), power electronic devices and its associated controllers as shown in Fig. 1.

Small signal stability model of WECS can be represented by the mathematical equations as given by (1). The detailed modeling procedure of WECS based on PMSG can be found in [13–15].

$$\begin{aligned} \frac{d\omega_g}{dt} &= \frac{\tau_e - \tau_{wg}}{J_{eq}} - \frac{B_m}{J_{eq}} \omega_g \\ \frac{di_d}{dt} &= \frac{1}{L_{ds} + L_{is}} (-R_s i_d + \omega_e (L_{qs} + L_{is}) i_q + u_d) \\ \frac{di_q}{dt} &= \frac{1}{L_{qs} + L_{is}} (-R_s i_q + \omega_e [(L_{ds} + L_{is}) i_q + \psi_f] + u_d) \\ \omega_e &= p\omega_g \\ \tau_e &= 1.5p((L_{ds} + L_{is}) i_d i_q + i_q \psi_f) \end{aligned} \quad (1)$$

where  $\omega_g$  is mechanical angular speed of generator and  $B_m$  corresponds to damping coefficient.  $\tau_{wg}$  represents aerodynamic torque. While  $\tau_e$ , and  $J_{eq}$  are electromechanical torque and equivalent inertia, respectively. Generator parameters corresponding to stator resistance ( $R_s$ ), leakage inductances ( $L_{id}, L_{iq}$ ), generator inductances ( $L_{d}, L_{q}$ ), electrical

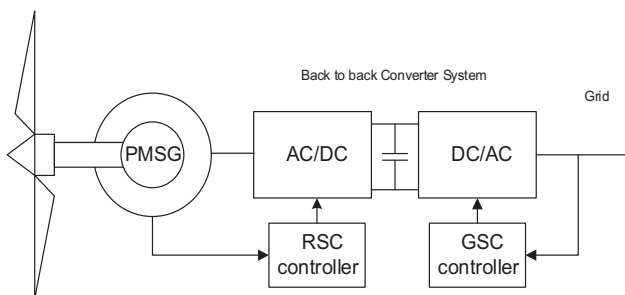


Fig. 1. Electrical scheme of WECS based on PMSG [13–15].

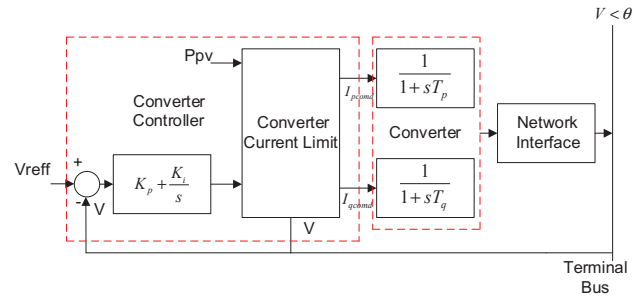


Fig. 2. A dynamic model of large-scale PV plant.

rotating speed ( $\omega_e$ ), magnetic flux ( $\psi_f$ ) and some poles ( $p$ ) are considered in this model. The sub-index  $g$  described the parameter of generator side [13–15].

### 2.2. PV plant model

A dynamic model of large scale PV plant consists of PV array, converter, and associated controller. The generated power from PV array is processed through the converter, which is employed as an interface device between PV array and the network. PV controller is responsible for producing an appropriate power to the grid [16,17]. A small signal model of large-scale PV power plant is depicted in Fig. 2. There are two main parts of the PV model: converter and associated controller [16–19]. The converter can be represented as a set of first-order differential equations corresponded to the aggregated model of inverter dynamic and low pass filter. The proposed control system consists of converter limit, PI controller, and reactive power control. Due to slow response, MPPT of PV plant can be assumed as a constant value. The detailed dynamic model of PV can be found in [20].

### 2.3. Battery energy storage model

In this paper, BES system has been examined to assess its influences on the small signal stability performance. Fig. 3 illustrates the block diagram of BES system. Several parameters corresponding to maximum DC voltage of batteries ( $E_{do}$ ), battery overvoltage ( $E_{b1}$ ), average DC voltage of the battery ( $E_{bt}$ ) and battery open circuit voltage ( $E_{boc}$ ) are considered. Here,  $I_{BES}$  and  $P_{BES}$  represent DC current through the battery and active power from the battery, respectively. Other parameters are relating to connecting resistance ( $r_{bt}$ ), battery internal resistance ( $r_{bs}$ ), self-discharge resistance ( $r_{bp}$ ), over voltage resistance ( $r_{b1}$ ), rotor speed deviation ( $\Delta\omega$ ), and commutating reactance ( $X_{co}$ ). While  $K_b$  and  $T_b$  are control loop gain and time constant, respectively [21–23].

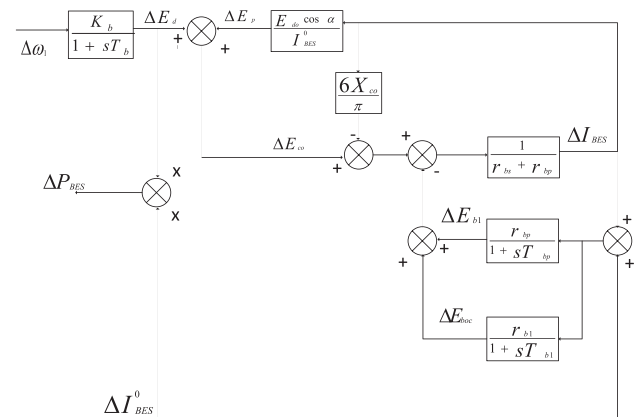


Fig. 3. Block diagram of BES system.

### 2.4. Power system model

Small signal model of power system comprises a set of linearized equations of nonlinear differential and algebraic equations (DAE). In this study, single machine infinite bus and multi-machine models will be developed to investigate the dynamic behavior of local power plant (local modes) and global power plants (local and inter-area modes) respectively [24]. A nonlinear mathematical model of the power system can be captured by (2) and (3) [25].

$$\dot{x} = f(x,y,u) \tag{2}$$

$$0 = g(x,y) \tag{3}$$

where  $x$  and  $y$  represent state and algebraic variables respectively. Machine and the associated controller is included in the differential equations while load flow and other network equations are included in algebraic equations [24].

## 3. Low-frequency oscillation and interaction in power system

### 3.1. Low-frequency oscillation

Low-frequency oscillation can be categorized as small disturbance rotor angle stability [6]. This stability is defined as the ability of power system to maintain stable condition after being subjected to small disturbance [26]. Low-frequency oscillation can be classified as a local and global mode or inter-area mode [27]. The local mode has a frequency around 0.7–2 Hz [27]. While the inter-area mode is associated with the generator in one area oscillates against another machine from another area, has a frequency range around 0.1–0.7 Hz [27].

Low-frequency oscillation can be examined by monitoring system eigenvalues of the reduced system state matrix. The eigenvalues will reflect various modes in the system, including oscillatory and non-oscillatory. State space representation of the system can be determined using (4), which can be obtained by linearizing (2) and (3) [28–30].

$$\begin{bmatrix} \Delta\dot{x} \\ 0 \end{bmatrix} = \begin{bmatrix} A & B \\ C & D_{21} \ J_{LF} \end{bmatrix} \begin{bmatrix} \Delta x \\ \Delta y \end{bmatrix} + E[\Delta u] \tag{4}$$

where  $\Delta x$  is a vector of state variables.  $\Delta y$  represents a vector of algebraic variables.  $\Delta u$  corresponded to the input vector.  $J_{LF}$  is the load-flow Jacobian.  $A$  and  $B$  are plant and control or input matrix respectively. While output and feedforward matrix are denoted by  $C$  and  $D$ , respectively. Furthermore, the reduced system state matrix of the entire system can be defined using (5) [29].

$$A_{sys} = \left( A - B \left[ \begin{pmatrix} D_{11} & D_{12} \\ D_{21} & J_{LF} \end{pmatrix}^{-1} \right] C \right) \tag{5}$$

The eigenvalue of the system matrix carries information about the stability of the system. Complex eigenvalue indicates frequency oscillation ( $f$ ) and damping ratio ( $\xi$ ) which can be described as given in (6), (7), and (8) [28,31–33].

$$\lambda_i = \sigma_i \pm j\omega_i \tag{6}$$

$$f_i = \frac{\omega_i}{2\pi} \tag{7}$$

$$\xi = \frac{-\sigma_i}{\sqrt{-\sigma_i^2 + -\omega_i^2}} \tag{8}$$

Participation factor is the method to measure state variable contribution in a specific mode and determine how each state variables affect the dynamic behavior of the corresponding mode [34]. Participation factor can be determined using (9) [31,34]

$$P_{ij} = \phi_{ij} \psi_{ij} \tag{9}$$

where  $\phi$  and  $\psi$  represent the right and left eigenvector, respectively. The product of right and left eigenvector provides dimensionless net participation of the state variables in a specific modes.

### 3.2. Modal interaction in power system

From low-frequency oscillation point of view, interaction among eigenvalues could be defined as a coincidence of two eigenvalues. Strong and weak interaction can be classified whether linearization is diagonalizable or not diagonalizable [31,35]. If the linearization is diagonalizable at the interaction, it is called as a strong interaction. If the linearization is not diagonalizable at the interaction point, it is called a weak interaction. Near a strong interaction, the participating eigenvalues are very sensitive to parameter variation. The trajectories of approaching eigenvalues significantly change due to strong interaction. The eigenvalue potentially moves towards the right half plane due to strong modal interaction. Moreover, in a particular case, two real eigenvalues become one complex eigenvalue and it can lead to unstable condition [31,35,36]. Weak interaction influences the damping performance of the particular modes. Furthermore, if this interaction is strong enough, the system may lead to less damped oscillatory conditions [31,35,37].

Interaction in a power system emerges due to a perturbation on increasing loading in a tie line, a variation of a power system’s parameter and machine’s inertia [31,35]. Power system interaction can be detected by analyzing the trajectories of suspected modes with the variation of a power system’s parameters. To confirm the occurrence of interaction, participation factor analysis of the associated modes has to be conducted. If the participation factor of a particular mode participated each other significantly, it could be expected that an interaction event had occurred [29].

### 3.3. Differential evolution algorithm

Differential evolution algorithm (DEA) was first introduced by Storn and Prince in 1997 [38]. This algorithm has five important step which are initialization, mutation, recombination, crossover, and selection [38]. In the initialization process, the initial value is determined randomly in certain areas, which have upper and lower limits, determined by the parameters to be optimized. The purpose of mutating and recombination is to produce a population of NP vector trail. The purpose of crossover is to form a vector crossover trail of the parameter value, which is duplicated on two different vectors, namely, the initial vector and vector mutant. Selection step is to determine the vector, that will be the population for the next iteration [38,39].

## 4. Results and discussions

Several case studies are reported in this paper in an attempt to investigate the influence of BES on the low-frequency oscillatory condition of a power system due to increasing penetration of RESs. Case studies were carried on MATLAB/SIMULINK environmental. Observation of trajectories of the critical modes was conducted to identify the interaction of investigated mode due to the variation of BES’s gain controller. Participation factor analysis was then conducted to obtain the contribution of important state variables in a particular mode. Finally, time domain simulation was conducted to validate the eigenvalue trajectories and to observe the effect of the interactions.

### 4.1. Case study 1

A single machine infinite bus (SMIB), popularly known as “Philip-Heffron” model, was used as a first test system as shown in Fig. 4. This SMIB system consists of a generator, represented in ninth order model, equipped with an exciter and governor [40]. An aggregated BES system was connected to bus load. In this study, it was considered that BES

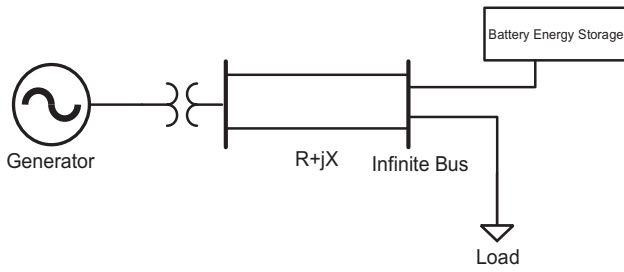


Fig. 4. SMIB with BES installed at bus load.

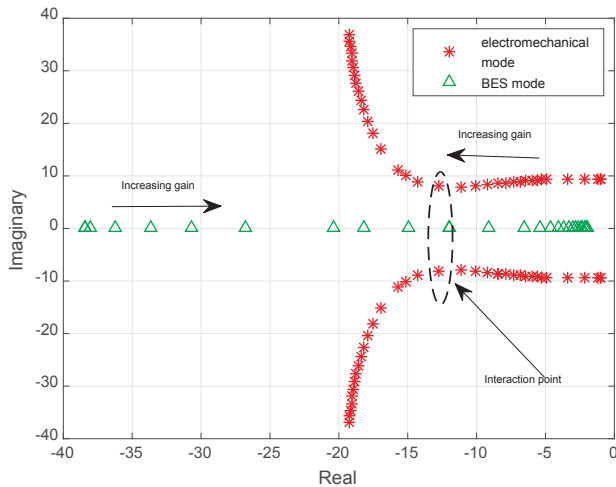


Fig. 5. Trajectories of electromechanical mode and BES mode.

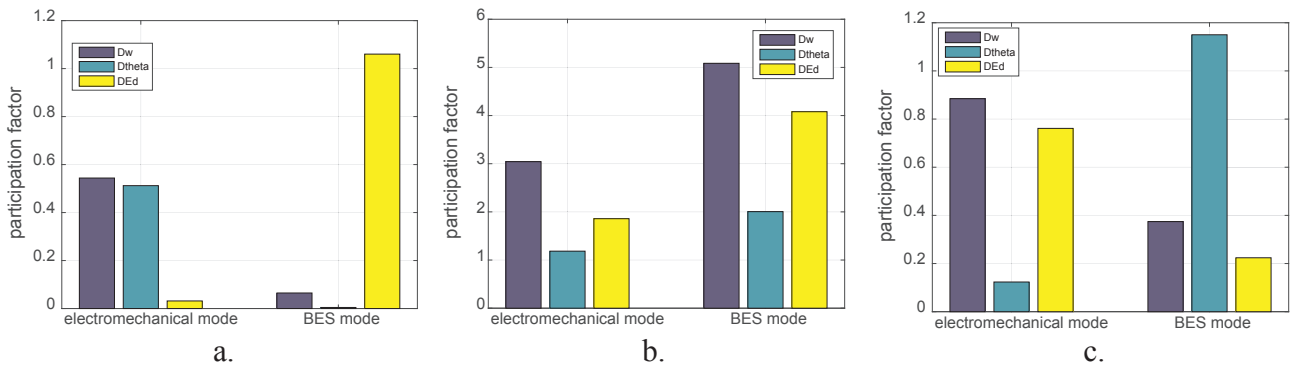


Fig. 6. Participation factor of electromechanical mode and BES mode. a. Far from interaction point; b. At the interaction point. c. After the interaction point.

only injected active power to the system. The gain of BES’s controller was varied in the range of 0.05–100 based on the maximum and minimum value of BES’s gain controller reported in [23].

Fig. 5 depicts the eigenvalue trajectories of critical modes due to the BES gain controller variation. As the BES gain increased from 0.05 to 27, the trajectories of electromechanical modes moved to the left-half plane. Conversely, the trajectories of critical modes corresponded to BES state variables moved towards the right-half plane. An interaction between electromechanical and BES modes emerged when the proportional gain controller was set at 27. The interacting modes were moving close each other during the interaction event. After the interaction, BES mode continuously moved towards the right-half plane while the imaginary parts of the electromechanical mode increased significantly. Without BES installation, typically the electromechanical mode move towards left half plane for any parameter variation (exciter gain or increasing loading). Hence the imaginary parts remain steady with the parameter variations. However, this engaged eigenvalues

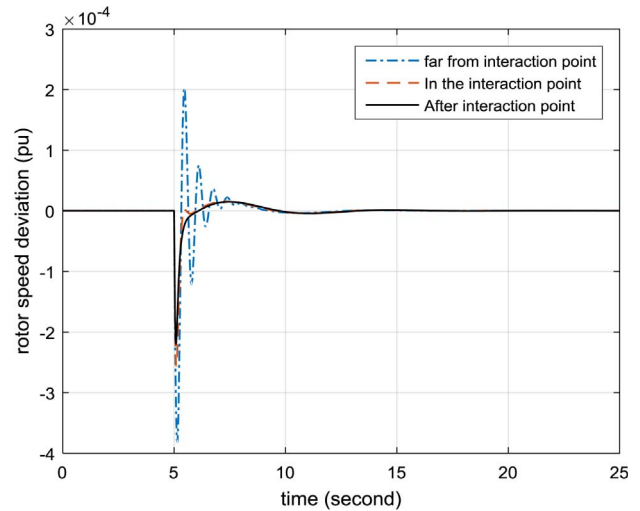


Fig. 7. The oscillatory condition of SMIB rotor speed.

movements deviated significantly when BES installed in the bus load. After a certain point, the electromechanical mode (red<sup>1</sup>) interacted with BES mode (green), result in increasing of electromechanical mode imaginary part and real part remained constant.

To confirm the occurrence of interaction, participation factor analysis was then conducted. Participation factor of the electromechanical ( $D_w$ ,  $D_{theta}$ ) and BES modes ( $D_{ed}$ ) due variation of the gain of a BES controller are illustrated in Fig. 6a–c. It was monitored that when the BES gain controller was tuned at 5 (far from interaction point) the participation factor of  $D_{ed}$  in electromechanical mode and  $D_{theta}$  in BES modes were relatively small as shown in Fig. 6a. As two interacting

modes came closer to a particular interaction point (with BES’s gain controller of 27), the contribution of those two state variables increasing significantly and reached the highest value as depicted in Fig. 6b). It was also noticeable that after leaving an interaction point, the participation factor decreased significantly as presented in Fig. 6c.

Time domain simulation was carried out to validate the eigenvalues trajectories. Excitation of the sensitive eigenvalues is realized by applying a small perturbation in the system in term of 0.05 step input of load. Figs. 7 and 8 illustrate the dynamic response of rotor speed and BES voltage respectively. It was observed that far from the interaction point as shown in Figs. 7 and 8, rotor speed was characterized by high overshoot while in BES voltage overshoot was relatively small. After the interaction point the pattern change, rotor speed overshoot relatively

<sup>1</sup> For interpretation of color in Figs. 5 and 11, the reader is referred to the web version of this article.

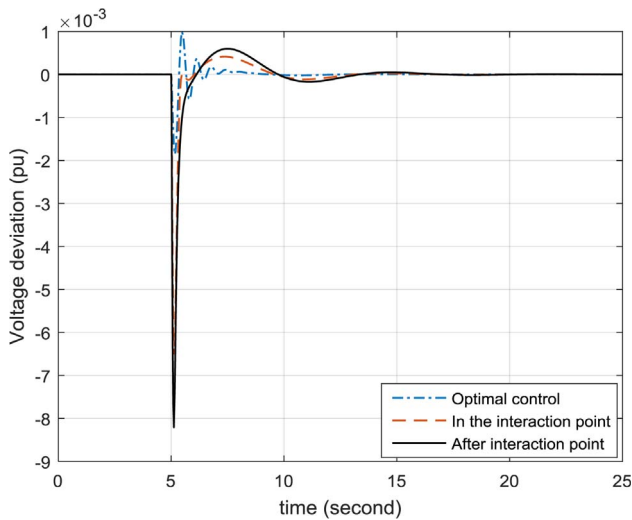


Fig. 8. The oscillatory condition of BES voltage.

small while overshoot of the BES voltage increase significantly. It means that increasing of BES gain controller can lead to eigen-interaction which resulted in deterioration of system damping. From this case study, it was found that BES system could influence the occurrence of power system interaction.

To mitigate the interaction between the investigated modes and to obtain the optimal system damping performance, parameter tuning of BES system’s controller was crucial. Hence, metaheuristic algorithm could be used to tune BES system’s controller. DEA method was applied in this study with considering maximum damping values as the objective function. From the DEA method, it was observed that the optimal system damping performance and mitigation of eigenvalues interaction were obtained when BES gain was tuned at 26.312. Fig. 9 shows the phase portrait of BES voltage against rotor angle after tuning process using DEA method. It was found that DEA method can damp the overshoot due to the interaction between electromechanical mode and mode from BES, indicated by smaller circular as shown in Fig. 9.

4.2. Case study 2

For providing more realistic study case, a multi machine power system is considered in the second study case. The 4-machine 12 buses two-area system popularly known as “Kundur” power system was

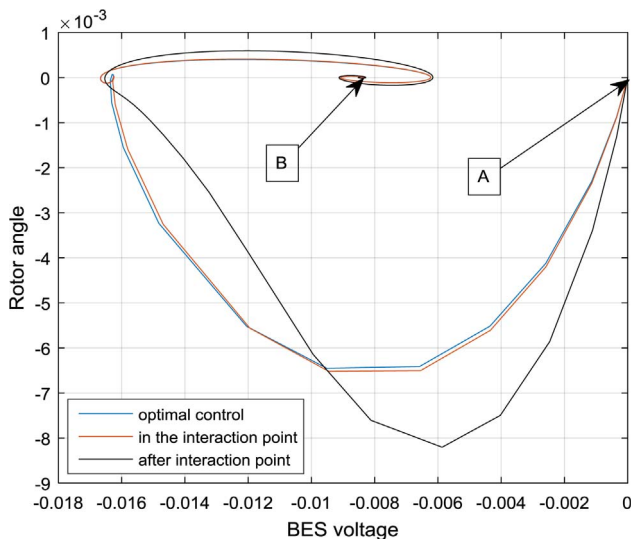


Fig. 9. Phase portrait of BES voltage after tuning with DEA.

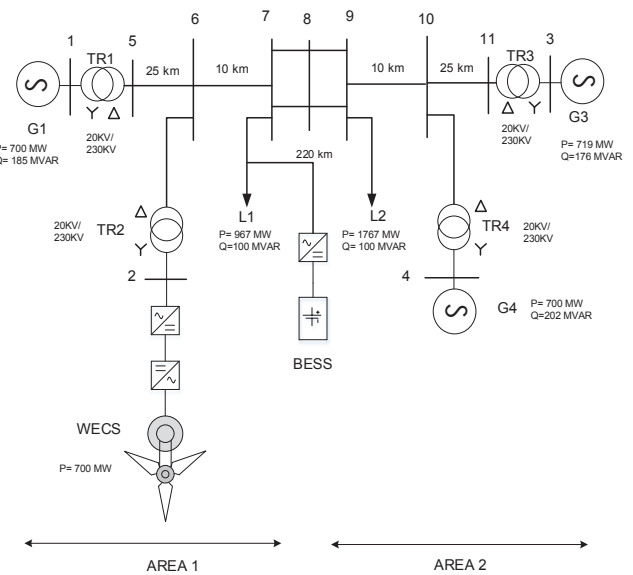


Fig. 10. Two-area power system with BES in bus load and WECS replacing generator 2.

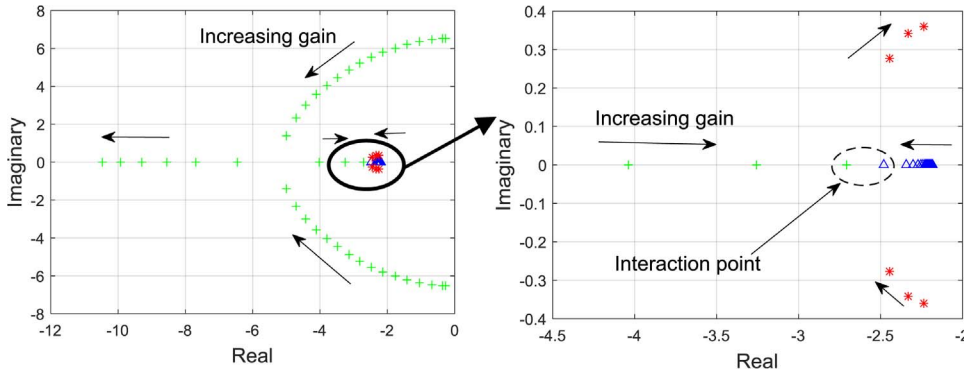
selected. A modification was made to the system by replacing generator 2 in area 1 with 700 MW WECS aggregated model (wind farm) and BES in load bus area 1 as shown in Fig. 10. In this study, it is considered that BES did not provide reactive power injection to the system. Moreover, it also assumed that WECS was operated at maximum power point condition. The modified system comprises of three synchronous machines and one WECS. Each synchronous generator was presented by a ninth order model equipped with the fast exciter and governor. The WECS was modeled by eleventh order model comprised of the wind turbine, drive train, permanent magnet synchronous generator, rotor, and grid side converter including the associated controller.

Table 1 shows eigenvalue and damping ratio comparison of two-area power system for replacing one synchronous generator with WECS. Replacing one synchronous generator with WECS resulted in a decrease of damping on the local mode of area 1 and the inter-area mode. It might have happened due to zero or inertia-less characteristic of WECS. Moreover, BES (with gain 40) could enhance the dynamic system performance in small signal stability indicated by higher damping value. However, BES could potentially has a negative impact in term of modal interaction. In the second study case, the small signal stability analysis was focused on power system interaction between local modes of area 1 and mode from WECS due to the variation of BES’s proportional gain controller.

Fig. 11 illustrates the impact of BES’s controller gain variation on local modes of area 1 and mode from WECS. Different to the first case study, in the second study case, interaction has occurred between local mode of area 1 and mode from WECS. This condition could have happened due to the different test system, different number of the state variable (in second case study the state variable was 41), and high penetration of large scale WECS. As the gain increased from 0.05 to 70, the trajectories of local mode of area 1 moved to the left-half plane, and the imaginary parts decreased gradually. It was found that after gain was set at 70, the complex local mode disappeared and eventually transformed into two real modes. One of this mode departed to the left-half plane, and the other moved to the right-half plane. It was also found that after gain was tuned at 85, one mode from local area 1 (green) that moved to the left half plane and interacted with mode from WECS (blue). The Strong interaction between those two modes occurred. Due to that interaction, mode from WECS and local mode from area 1 aligned at a certain point, resulting in a novel complex mode (red) which moved towards the right-half plane as shown in the second eigenvalue plot in Fig. 11. The new mode was associated with state

**Table 1**  
Eigenvalue and damping comparison of the cases.

Cases	Modes					
	Local 1		Local 2		Inter-area	
	Eigen	Damp.	Eigen	Damp.	Eigen	Damp.
Base case	$-0.325 \pm 6.758i$	0.048	$-0.341 \pm 7.018i$	0.049	$-0.07 \pm 2.609i$	0.026
With WECS	$-0.278 \pm 6.539i$	0.043	$-0.07 \pm 2.609i$	0.049	$-0.05 \pm 2.911i$	0.017
With BES	$-3.143 \pm 4.867i$	0.543	$-0.341 \pm 7.013i$	0.049	$-0.43 \pm 3.164i$	0.135



**Fig. 11.** Trajectories of local mode area 1 and mode from WECS due to the variation of BES gain controller.

**Table 2**  
Detailed features of the new mode.

Kbes	Mode	Damping	f (Hz)	State variable
90	$-2.4454 \pm 0.2760i$	0.99	0.044	WECS Id and $D_w, D_{theta}$ G1
95	$-2.3298 \pm 0.3407i$	0.98	0.054	WECS Id and $D_w, D_{theta}$ G1
100	$-2.2350 \pm 0.3597i$	0.98	0.057	WECS Id and $D_w, D_{theta}$ G1

variables from WECS and local modes area 1. The detailed features of the new mode is illustrated in Table 2.

Participation factor of the local mode of area 1 and mode from WECS under variation of BES gain is depicted in Fig. 12a–c. It was found that when the BES gain controller was tuned at 75 (far from interaction point) the participation factor of rotor speed ( $D_w$ ), rotor angle ( $D_{theta}$ ) and WECS current ( $I_d$ ) state variables in the engaged modes were relatively small as shown in Fig. 12a. At the interaction point (BES’s controller gain is 85) participation factor of those state variables in local mode and mode from WECS reached the highest value as depicted in Fig. 12b. It was also noticeable that after interaction point the participation factor started to decrease as presented in Fig. 12c. It was noticeable that participation factor of local mode from area 1 and mode from WECS had the same value, it happened since

after the interaction of the two modes become one complex conjugate mode.

Time domain simulations were carried out to verify and validate the eigenvalue trajectories. To observe the dynamic response, a small disturbance was made in the system by giving 0.05 step input change to the load. Fig. 13a–c illustrate time domain simulations of rotor speed response in generator 1, direct axis current of WECS and electro-mechanical torque of WECS. The detailed features and overshoot of time domain simulation results presented in Fig. 13a–c are summarised in Table 3. It was noticeable that the oscillatory condition of the system far from interaction was more damped than near to the interaction point. The worst condition is monitored after the interaction took place, due to the appearance of a new complex conjugate modes appeared. It was also found that interaction between WECS and local mode of area 1 did not give any significant influences in the oscillatory condition of generator 1. Although one mode moved to the right-half plane, another mode moved to the left-half plane. Hence the oscillatory condition was more damped after the interaction.

To mitigate the interaction between the investigated modes and to obtain the optimal system damping performance, parameter tuning of BES system’s controller was crucial. DEA method was applied in this study with considering maximizing damping value as the objective

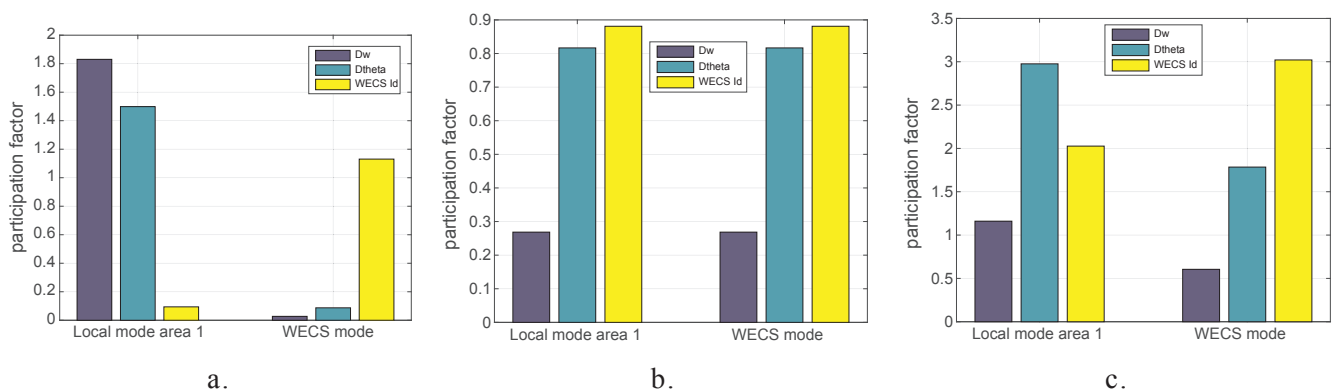


**Fig. 12.** Participation factor of electromechanical mode and mode from WECS. a. Far from interaction point; b. At the interaction point. c. After the interaction point.

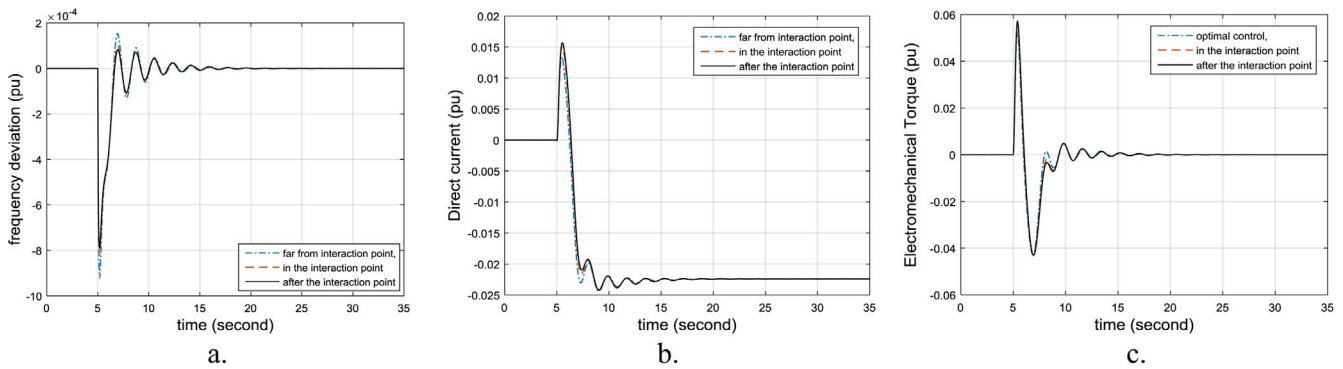


Fig. 13. The oscillatory condition of different cases. a. Generator 1 rotor speed. b. WECS's direct axis current. c. Electromechanical torque.

Table 3  
Detailed features of overshoot and settling time.

		Far from interaction	In the interaction point	After the interaction
Generator 1	Overshoot (pu)	-0.0009229	-0.0008239	-0.0007906
	Settling time (s)	> 15	> 15	> 15
WECS's direct axis current	Overshoot (pu)	0.01339	0.01505	0.01568
	Settling time (s)	> 15	> 15	> 15
Electromechanical torque	Overshoot (pu)	0.05246	0.05597	0.05721
	Settling time (s)	> 15	> 15	> 15

function. From the DEA method, it was reported that the optimal system damping performance and mitigation of eigenvalues interaction were obtained when BES gain was tuned at 76.754. Fig. 14 shows the phase portrait of rotor speed of WECS against WECS electromechanical response after tuning process using DEA method. It was found that by using DEA method can damp the overshoot due to the interaction between electromechanical mode and mode from BES, indicated by smaller circular as shown in Fig. 14.

4.3. Case study 3

PV power plant might introduce a different dynamic to the power system. Hence, it is necessary to investigate the impact of PV power plant. The Two-area test power system was further modified to provide an investigation of BES impact on power system small signal stability performance. Generator 2 from area 1 was replaced with 350 MW PV. Furthermore, a WECS plant with a capacity of 350 MW was connected to the grid at bus 6 as shown in Fig. 15. The modified system consists of

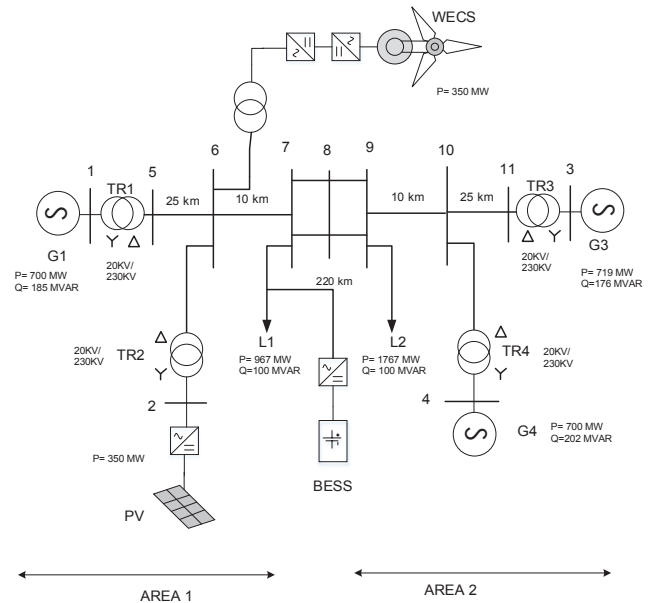


Fig. 15. Two-area power system with BES in bus load and WECS and PV replacing generator 2.

three synchronous machines, one WECS, one PV plant and one BES in bus load area 1. It was assumed that WECS and PV operated at maximum power point condition while BES only injected active power to the system. The synchronous generator in the system was presented by ninth order model with fast exciter and governor. The WECS was modeled by eleventh order model consists of the wind turbine drive train, permanent magnet synchronous generator, rotor and grid side converter including the associated controller. The PV comprised of the converter and associated controller was modeled into the sixth order differential equation.

Table 4 shows the system eigenvalues for replacing one synchronous generator with WECS and PV. Replacing one synchronous generator with WECS and PV plants resulted in a decrease of damping on the local

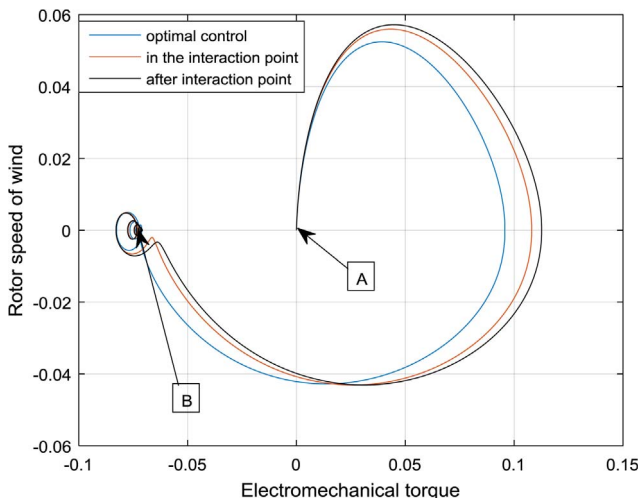
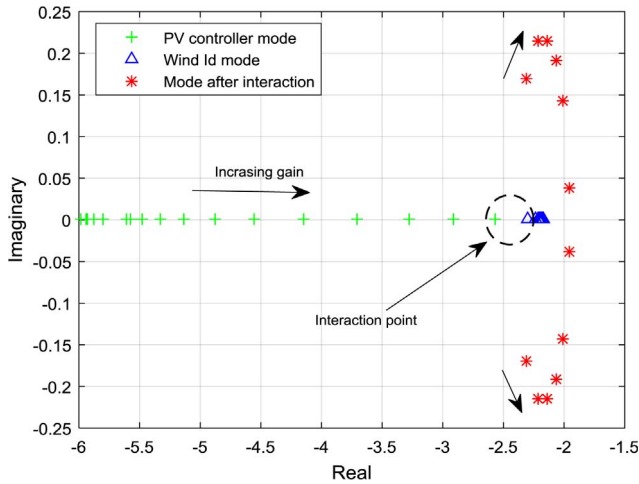


Fig. 14. Phase portrait of WECS's with optimal control of BES for second study case.

**Table 4**  
Eigenvalue and damping comparison of the cases.

Cases	Modes					
	Local 1		Local 2		Inter-area	
	Eigen	Damp.	Eigen	Damp.	Eigen	Damp.
Base case	$-0.325 \pm 6.758i$	0.048	$-0.341 \pm 7.018i$	0.049	$-0.07 \pm 2.609i$	0.026
With WECS	$-0.283 \pm 6.582i$	0.043	$-0.341 \pm 7.018i$	0.049	$-0.03 \pm 3.025i$	0.011
With BES	$-3.730 \pm 4.948i$	0.638	$-0.341 \pm 7.011i$	0.049	$-0.33 \pm 3.410i$	0.096



**Fig. 16.** Trajectories of PV mode and WECS mode due to the variation of BES gain controller.

**Table 5**  
Detailed features of the new mode.

Kbes	Mode	Damp.( $\zeta$ )	f (Hz)	State variable
75	$-2.314 \pm 0.168i$	0.98	0.027	PV controller ( $\epsilon$ ), WECS $I_d$
80	$-2.217 \pm 0.214i$	0.97	0.034	PV controller ( $\epsilon$ ), WECS $I_d$
85	$-2.136 \pm 0.215i$	0.99	0.034	PV controller ( $\epsilon$ ), WECS $I_d$
90	$-2.068 \pm 0.190i$	0.99	0.030	PV controller ( $\epsilon$ ), WECS $I_d$
95	$-2.010 \pm 0.143i$	0.98	0.023	PV controller ( $\epsilon$ ), WECS $I_d$
100	$-1.960 \pm 0.037i$	0.99	0.006	PV controller ( $\epsilon$ ), WECS $I_d$

mode of area 1 and inter-area mode. It has happened due to zero or inertialess and different dynamic characteristic of WECS. Moreover, BES (with gain 40) could enhance the system dynamic indicated by higher damping value. However, BES could potentially has a negative impact in terms of modal interaction.

The third study case was focused on power system interaction between modes from PV plant and WECS due to the variation of BES's

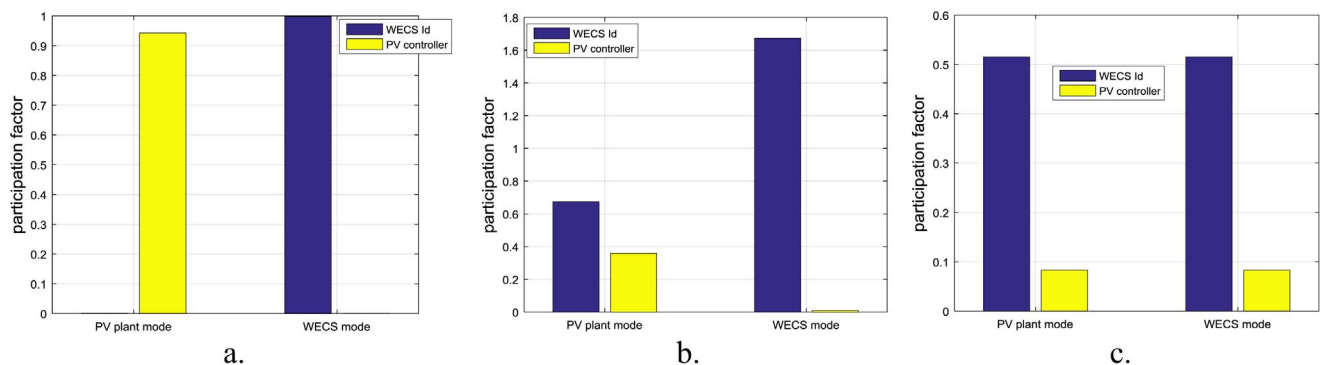


**Fig. 17.** Participation factor of mode from PV and mode from WECS. a. Far from interaction point; b. At the interaction point. c. After the interaction point.

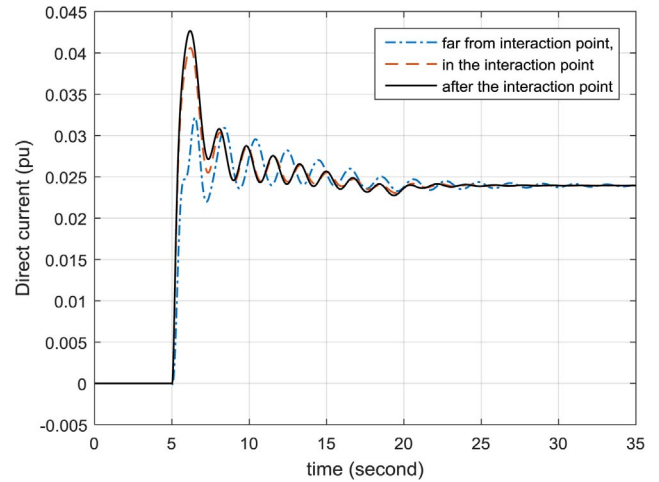


**Fig. 18.** The oscillatory condition of WECS's direct axis current.

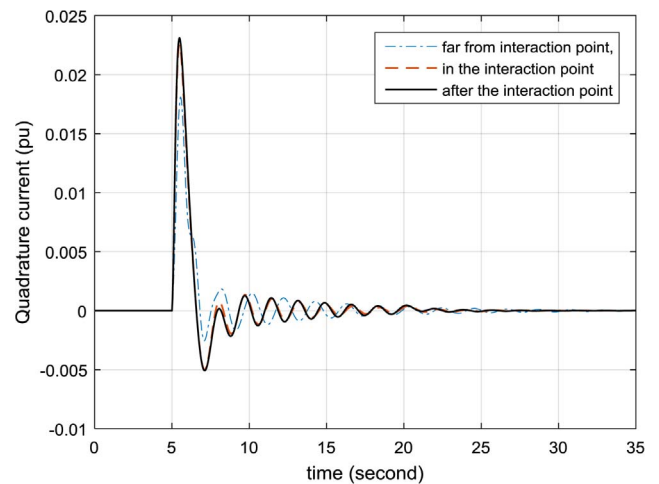


**Fig. 19.** The oscillatory condition of WECS's quadrature axis current.

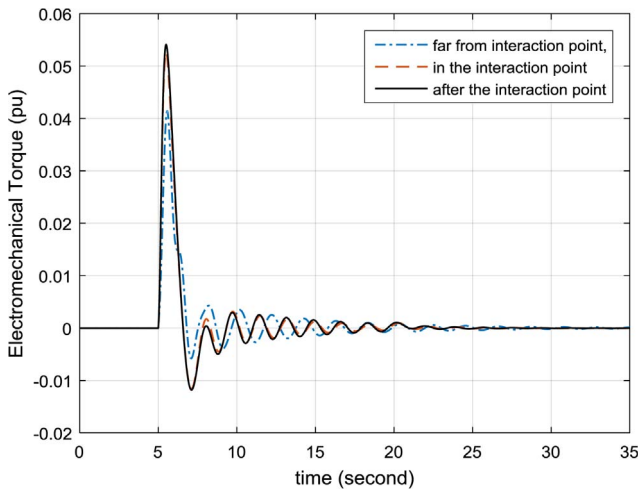


Fig. 20. The oscillatory condition of WECS's electromechanical torque.

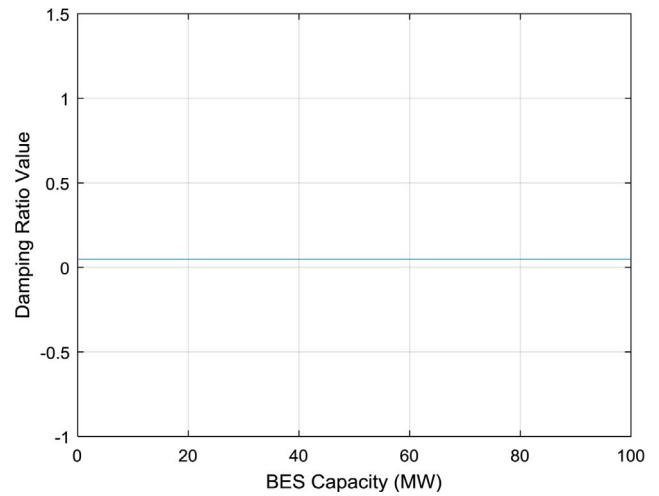


Fig. 23. Damping value of local mode area 2 due to BES capacity.

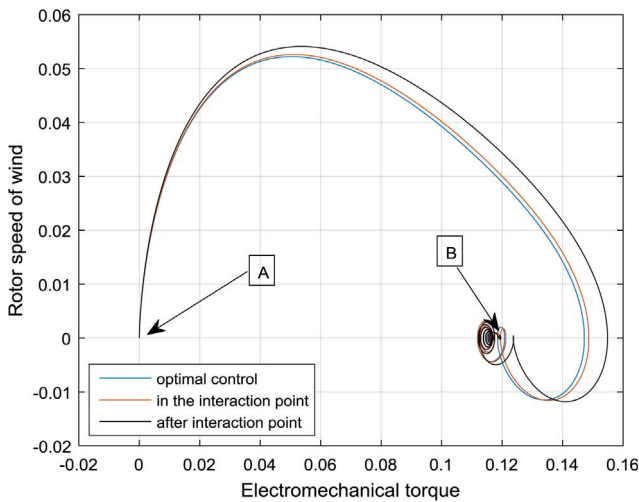


Fig. 21. Phase portrait of WECS's with optimal control of BES for the third study case.

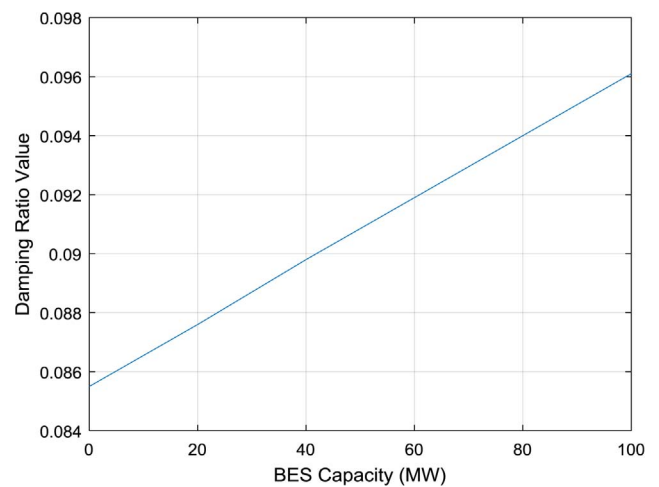


Fig. 24. Damping value of inter-area mode due to BES capacity.

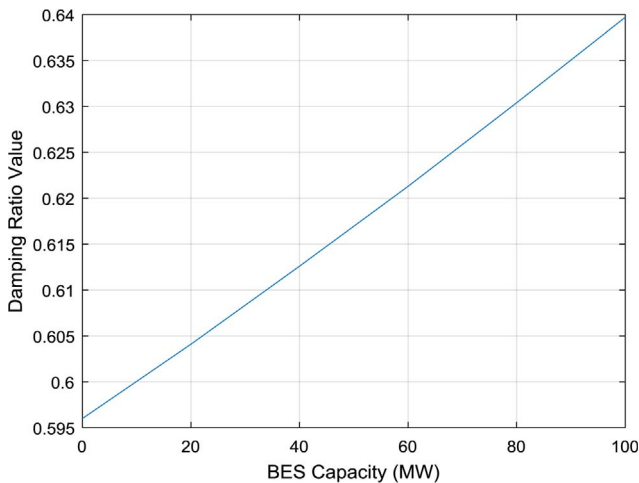


Fig. 22. Damping value of local mode area 1 due to BES capacity.

proportional controller gain. Fig. 16 illustrates the impact of BES's gain controller on sensitive modes from WECS and PV plant. As the BES gain increased from 0.05 to 70, the trajectories of PV mode departed to the right-half plane while mode from WECS moved to the left-half plane. It was found that after BES gain was set at 70, the strong interaction

between mode from PV plant and mode from WECS emerged. It was also monitored that after the interaction, mode from PV plant and mode from WECS aligned and transformed into a new mode. It was happened due to the variation of BES's gain resulting interaction between mode from PV and mode from WECS. The detailed features of the new mode was illustrated in Table 5.

Participation factor of the mode from PV plant and mode from WECS due variation of BES are depicted in Fig. 17a–c. Different with case study 2, in this case study the interaction emerged between mode from PV plant and mode from WECS. This condition could have happened due to different dynamic characteristic and different number of state variable (in this case study the number of state variable was 47). Moreover, this case study also consider two different type of RESs (PV and WECS). It was found that when the BES's gain was 10 (far from interaction point) the participation factor of WECS current ( $I_d$ ) and PV controller ( $\epsilon$ ) state variables were relatively small as shown in Fig. 17a. At the interaction point (BES's gain is 75) contributions of those state variables in both of interacting modes reached the highest value as depicted in Fig. 17b. It was also noticeable that after interaction point the participation factor of the corresponded state variables started to decrease as presented in Fig. 17c. It was noticeable that participation factor of mode from PV plant and mode from WECS have the same value, it emerged since after the interaction event the two modes become one complex conjugate mode.

Effects of modal interaction between WECS and PV on electro-mechanical torque and current of WECS is observed by applying a small

**Table 6**  
Eigenvalue and damping comparison of the cases.

BES Location	Modes					
	Local 1		Local 1		Inter-area	
	Eigen	Damp.	Eigen	Damp.	Eigen	Damp.
Area-1	$-3.730 \pm 4.948i$	0.63	$-0.341 \pm 7.01i$	0.04	$-0.33 \pm 3.410i$	0.096
Area-2	$-0.368 \pm 6.776i$	0.05	$-2.503 \pm 6.04i$	0.38	$-0.34 \pm 3.069i$	0.109
Middle	$-1.456 \pm 6.352i$	0.22	$-0.350 \pm 6.977i$	0.05	$-0.92 \pm 3.244i$	0.271

load disturbance to the generator 1 by giving 0.05 step input. Figs. 18–20 illustrate time domain simulation of d-q axis current and electromechanical torque from WECS. It was observed that far from interaction point, the WECS direct and quadrature axis current ( $I_d$ ,  $I_q$ ) and electromechanical torque of WECS had the smallest overshoot and fastest settling time. In the interaction point, the overshoot of three signal above increased significantly, and also have the more oscillatory condition. The worst oscillatory condition occurred after interaction point, indicated by higher overshoot and longer setting time of dynamic system response.

The appropriate method to tune BES's gain controller is crucial. In here, DEA was chosen as optimization method for tuning BES system's controller. To get the best parameter maximum damping value of the system was chosen as objective function subject to BES's gain minimum and maximum value. From the DEA method, it was reported that the optimal system damping performance and mitigation of eigenvalues interaction were obtained when BES gain was tuned at 73.589. Fig. 21 shows the phase portrait of rotor speed of WECS against WECS electromechanical response after tuning process using DEA method. It was found that DEA method can damp the overshoot due to the interaction between electromechanical mode and mode from BES, indicated by smaller loops as shown in Fig. 21.

Figs. 22 and 24 show the damping performance of local mode in area 1 and inter-area mode. It was observed that by increasing BES capacity, the damping performance of local mode in area 1 and inter-area mode increased gradually. This condition could have happened due to injected active power from BES to the load that reduces the stress of generator 1. Fig. 23 shows the damping performance of local mode area 2 due to increasing BES capacity. It was monitored that the damping performance of local mode of area 2 remains in its position. It was noticed that the proximity of BES play important role in the dynamic performance of the system.

Table 6 illustrates the eigenvalue and damping performance of the system for different locatio of BES. It was monitored that when BES is installed in area 2 the damping performance of local mode of area 2 increased significantly. While, the damping performance of local mode of area 1 increased moderately. This condition could have happened due to the change of power flow condition before and after BES installation. When the BES installed in area 2, the power flow from area 1 to area 2 is decrease proportionally. The decreasing power flow from area 1 to area 2 reduces the stress of generator in area 1. A similar pattern was observed in inter-area mode, due to the decreasing of powerflow from area 1 to area 2, the stress in the transmission line is also decreased. Therefore, the damping performance of inter-area mode increased significantly. Moreover, when BES was installed in the middle of the transmission line, the damping performance of three modes enhanced.

## 5. Conclusions

This paper investigates the possible impact of BES system in a power system small signal stability and modal interaction considering high penetration of RESs. From the investigated study cases, it was found that BES could enhance the damping performance of the system

significantly (from 4% to 60% for local mode area 1 and 1–10% for inter-area mode) even though one synchronous generator has been replaced by inertia-less RESs. It was monitored that BES proximity has significant influenced on system dynamics (no significant impact on local mode of area 2). The variation of the gain of a BES controller has significantly influenced electromechanical mode of the synchronous machine, and modes coming from PV plant and WECS. The capacity of the BES has no significant influence on various electromechanical modes. However, location of the BES seems to have a significant influence on damping of the modes.

Moreover, a new complex conjugate mode emerged as a result of the interaction event between local mode of area 1 and WECS mode. When PV plant was integrated into the system, there is no interaction between local mode of area 1 and WECS mode was monitored. However, the interaction phenomena emerged between PV plant and WECS modes, resulting in a new complex conjugate mode. To improve the system damping and mitigate the modal interaction, DEA optimization method is used. Further research is required to utilizing power system stabilizer (PSS) to avoid potential interactions and to avoid the unstable operating condition of power systems.

## Acknowledgments

The first author is very grateful to the Ministry of Finance of Indonesian Government for awarding him the Endowment Fund of Education Scholarship (LPDP) for his doctoral degree studies at the University of Queensland, Australia.

## Appendix A. Supplementary material

Supplementary data associated with this article can be found, in the online version, at <http://dx.doi.org/10.1016/j.ijepes.2017.11.021>.

## References

- [1] Shah R, Mithulananthan N, Bansal RC, Ramachandaramurthy VK. A review of key power system stability challenges for large-scale PV integration. *Renew Sustain Energy Rev* 2015;41(1):1423–36.
- [2] Jabr RA. Adjustable robust OPF with renewable energy sources. *IEEE Trans Power Syst* 2013;28:4742–51.
- [3] Yorino N, Abdillah M, Sasaki Y, Zoka Y. A method for evaluating robust power system security against uncertainties. In: 2016 International Seminar on Intelligent Technology and Its Applications (ISITIA); 2016. p. 497–502.
- [4] Lamichhane S, Mithulananthan N. Influence of wind energy integration on low frequency oscillatory instability of power system. 2014 Australasian Universities Power Engineering Conference (AUPEC). 2014. p. 1–5.
- [5] Lamichhane S, Mithulananthan N. Possible impact of large scale wind energy integration on small signal stability. 2015 IEEE PES Asia-Pacific Power and Energy Engineering Conference (APPEEC). 2015. p. 1–5.
- [6] Shah R, Mithulananthan N, Sode-Yome A, Lee K.Y. Impact of large-scale PV penetration on power system oscillatory stability. In: IEEE PES general meeting; 2010. p. 1–7.
- [7] Kalyani S, Nagalakshmi S, Marisha R. Load frequency control using battery energy storage system in interconnected power system. In: 2012 Third International Conference on Computing Communication & Networking Technologies (ICCCNT); 2012. p. 1–6.
- [8] Prajapati P, Parmar A. Multi-area load frequency control by various conventional controller using battery energy storage system. 2016 International Conference on Energy Efficient Technologies for Sustainability (ICEETS). 2016. p. 467–72.
- [9] Hung DQ, Mithulananthan N, Bansal R. Integration of PV and BES units in

- commercial distribution systems considering energy loss and voltage stability. *Appl Energy* 2014;113:1162–70.
- [10] Deeba SR, Sharma R, Saha TK, Chakraborty D, Thomas A. Evaluation of technical and financial benefits of battery-based energy storage systems in distribution networks. *IET Renew Power Gener* 2016;10:1149–60.
- [11] Shah R, Mithulananthan N. A comparison of ultracapacitor, BESS and shunt capacitor on oscillation damping of power system with large-scale PV plants. *AUPEC* 2011. 2011. p. 1–6.
- [12] Sui X, Tang Y, He H, Wen J. Energy-storage-based low-frequency oscillation damping control using particle swarm optimization and heuristic dynamic programming. *IEEE Trans Power Syst* 2014;29:2539–48.
- [13] Yin M, Li G, Zhou M, Zhao C. Modeling of the wind turbine with a permanent magnet synchronous generator for integration. *Power Engineering Society General Meeting*, 2007. *IEEE*; 2007. p. 1–6.
- [14] Rolan A, Luna A, Vazquez G, Aguilar D, Azevedo G. Modeling of a variable speed wind turbine with a permanent magnet synchronous generator. 2009 *IEEE International Symposium on Industrial Electronics*. 2009. p. 734–9.
- [15] Zou Y, He J. Comprehensive modeling, simulation and experimental validation of Permanent Magnet Synchronous generator wind power system. In: 2016 *IEEE/IAS 52nd Industrial and Commercial Power Systems Technical Conference (I&CPS)*; 2016. p. 1–9.
- [16] Shah R, Mithulananthan N, Lee KY. Design of robust power oscillation damping controller for large-scale PV plant. 2012 *IEEE power and energy society general meeting*. 2012. p. 1–8.
- [17] Shah R, Mithulananthan N, Lee KY. Large-scale PV plant with a robust controller considering power oscillation damping. *IEEE Trans Energy Convers* 2013;28:106–16.
- [18] Setiadi H, Krismanto AU, Mithulananthan N. Influence of BES system on local and inter-area oscillation of power system with high penetration of PV plants. In: 2017 *International Conference on Applied System Innovation (ICASI)*; 2017. p. 1–4.
- [19] Setiadi H, Krismanto AU, Mithulananthan N. Enabling BES in large PV plant for stability enhancement on power systems with high RES. In: 2017 *IEEE Innovative Smart Grid Technologies-Asia (ISGT-Asia)*, Auckland, New Zealand, 2017.
- [20] Clark K, Miller NW, Walling R. Modelling of GE solar photovoltaic plants for grid studies. *General Electrical International Inc*, Schenectady, NY; 2010.
- [21] Kerdphol T, Qudaih Y, Mitani Y. Battery energy storage system size optimization in microgrid using particle swarm optimization. In: *IEEE PES innovative smart grid technologies*, Europe; 2014. p. 1–6.
- [22] Kerdphol T, Fuji K, Mitani Y, Watanabe M, Qudaih Y. Optimization of a battery energy storage system using particle swarm optimization for stand-alone microgrids. *Int J Electr Power Energy Syst* 2016;81:32–9.
- [23] Setiadi H, Mithulananthan N, Hossain MJ. Impact of battery energy storage systems on electromechanical oscillations in power systems. In: 2017 *IEEE power and energy general meeting*, Chicago, USA; 2017.
- [24] Prasertwong K, Mithulananthan N, Thakur D. Understanding low-frequency oscillation in power systems. *Int J Electr Eng Educ* 2010;47:248–62.
- [25] Lastomo D, Setiadi H, Djalal MR. Optimization of SMES and TCSC using particle swarm optimization for oscillation mitigation in a multi machines power system. *J Mech Electric Power Veh Technol* 2017;8:11–21.
- [26] Krismanto AU, Nadarajah M, Krause O. Influence of renewable energy based microgrid on low frequency oscillation of power systems. 2015 *IEEE PES Asia-Pacific Power and Energy Engineering Conference (APPEEC)*. 2015. p. 1–5.
- [27] Kundur P, Paserba J, Ajarapu V, Andersson G, Bose A, Canizares C, et al. Definition and classification of power system stability IEEE/CIGRE joint task force on stability terms and definitions. *IEEE Trans Power Syst* 2004;19:1387–401.
- [28] Kundur P, Balu NJ, Lauby MG. *Power system stability and control*. vol. 7. New York: McGraw-hill; 1994.
- [29] Sauer PW, Pai M. *Power system dynamics and stability*. Urbana 1998.
- [30] Setiadi H, Jones KO. Power system design using firefly algorithm for dynamic stability enhancement. *Indonesian J Electric Eng Comput Sci* 2016;1:446–55.
- [31] Krismanto AU, Mithulananthan N, Krause O. Microgrid impact on low frequency oscillation and resonance in power system. In: 2016 *IEEE Innovative Smart Grid Technologies - Asia (ISGT-Asia)*; 2016. p. 424–9.
- [32] Lastomo D, Setiadi H, Faisal M, Ashfahani A, Bangga G, Hutomo G, et al. The effects of energy storage on small signal stability of a power system. In: 2017 *International Seminar on Technology and Its Application (ISITIA)*, Surabaya, Indonesia; 2017.
- [33] Taufik M, Lastomo D, Setiadi H. Small-disturbance angle stability enhancement using intelligent redox flow batteries. In: 2017 *4th international conference on Electrical Engineering, Computer Science and Informatics (EECSI 2017)*, Yogyakarta, Indonesia; 2017.
- [34] Hassan LH, Moghavvemi M, Almurib HA, Muttaqi K, Ganapathy VG. Optimization of power system stabilizers using participation factor and genetic algorithm. *Int J Electr Power Energy Syst* 2014;55:668–79.
- [35] Dobson I, Zhang J, Greene S, Engdahl H, Sauer PW. Is strong modal resonance a precursor to power system oscillations? *IEEE Trans Circ Syst I: Fundam Theory Appl* 2001;48:340–9.
- [36] Seyranian AP, Mailybaev AA. Interaction of eigenvalues in multi-parameter problems. *J Sound Vib* 2003;267:1047–64.
- [37] Krismanto A, Nadarajah M. Identification of modal interaction and small signal stability in autonomous microgrid operation. *IET Gener Transm Distrib* 2017.
- [38] Storn R, Price K. Differential evolution—a simple and efficient heuristic for global optimization over continuous spaces. *J Global Optim* 1997;11:341–59.
- [39] Lastomo D, Setiadi H, Djalal MR. Optimization pitch angle controller of rocket system using improved differential evolution algorithm. *Int J Adv Intell Informat* 2017;3.
- [40] Mado I, Soeprijanto A. Design of robust-fuzzy controller for SMIB based on power-load cluster model with time series analysis. In: *Electrical Power, Electronics, Communications, Controls and Informatics Seminar (EECCIS)*, 2014; 2014. p. 8–15.